Yeast driven self exfoliation and functionalisation of graphene

Reddhy Mahle[1], Swathi Suran[3], Appu Singh[2], Partha Kumbhakar[2], Douglas S Galvao[4], Venkata Ravi Sankar Cheela[5], Brajesh Dubey[6], R.R. Nair[3,], Chandra S Tiwary[2,*], Rintu Banerjee[1,*]*

[1]Agricultural and Food Engineering Department, Indian Institute of Technology, Kharagpur, West Bengal-721302 India

[2]Department of Metallurgical and Materials Engineering, Indian Institute of Technology Kharagpur, West Bengal-721302 India

[3]National Graphene Institute, University of Manchester, Manchester, UK

[4] Applied Physics Department, University of Campinas, Campinas, Brazil

[5] Department of Civil Engineering, MVGR College of Engineering (A), Vizianagaram, India

[6] Department of Civil Engineering, Indian Institute of Technology Kharagpur, West Bengal-721302 India

We report an eco-friendly, economical and green approach to synthesize few-layers of functionalised graphene from large graphite flakes and chunks without the aid of any external mechanical forces. Here, we demonstrate a fermentation process aided by friendly microbes like yeast to effortlessly exfoliate graphite to graphene with a high yield. The evident flaking and delamination of graphene layers, characterized using scanning electron microscopy (SEM), atomic force microscopy (AFM) and Raman spectroscopy, confirmed the successful exfoliation of graphite to few-layer graphene (~10 nm in thickness). The gate-to-gate life cycle assessment of the developed method identified the environmental hotspots of the process. The biofunctionalized graphene (as suggested by Fourier transform infrared (FTIR) spectroscopy) was explored for its application in NH_4^+ sensing, where it exhibited the limit of detection to be ~20 ppm. The detection mechanism was explained based on Raman and FTIR spectroscopy which revealed the functional state and lattice changes introduced in the graphene layers by NH_4^+ ions. Our study demonstrates a novel, cost-effective exfoliation of graphite using off-the-shelf materials in laboratories or kitchens and has the potential to be scaled up to industry levels. The yeast cells also exhibited their potential in flaking off the bulk MoS_2 structure into few-layer MoS_2 sheets.

Keywords: graphene, economical, green, dry yeast, ammonium ions detection, life cycle assessment

Research into two-dimensional (2D) materials has evolved in the last ten years from the lab-scale proof of concept to pilot-scale demonstrations.[1,2] One of the key challenges in converting the prototype to a product is the energy cost of 2D materials' production; since all of the material synthesis uses external energy sources such as electricity, chemicals, mechanical force etc., and limits to decrease the cost of the production.[1,3] However, there are several biological processes wherein nature produces compounds without the aid of external energy. For example, collagen in living species is produced without any external energy source.[4] Previously, there have been attempts to mimic such processes using yeast for the production of chiral centres etc.[5] However, such self-mediated natural processes have never been explored to produce 2D materials. Here, we report the self-exfoliation and functionalization of graphene by using yeast in the presence of glucose without any external energy source. We show that, in such a process, the yeast cells exert much-needed mechanical shear forces to exfoliate graphite from the edges. In addition to the self-exfoliation, this process produces ethanol during fermentation, which helps disperse the exfoliated graphene to form a colloidal dispersion.

Fig.1(a) demonstrates the schematic of the process used for the functionalized graphene production. Dry yeast cells were inoculated with graphite powder suspension in glucose solution at room temperature. The solution in the flask turned dark and turbid after one week when visually inspected, as seen in Fig. 1(b). On the other hand, no visible differences were noticed in the reference yeast glucose mixture without graphite and also the reference glucose graphite mixture solution without the yeast (Fig. 1b). The appearance of dark colloidal dispersion when yeast and graphite simultaneously present in glucose solution suggests exfoliation of graphite. As supporting evidence of exfoliation, we anchored thin graphite layers by mechanical exfoliation to an Si/SiO_2 (290nm) samples. As seen in Fig. 1(c), a few layer graphene (~10 layers, measured by optical contrast) was successfully seen to be delaminated when immersed inside yeast-glucose solution for 1 week. To further characterise the exfoliation of graphite in yeast-glucose dispersions, the samples were subjected to a differential centrifugation process to remove yeast, and thick graphite flakes (details given in Method section). The obtained suspensions were drop-casted on Si substrates for all further characterization. The AFM micrograph, Fig. 1 (d), showed the uniform distribution of graphene flakes where the thickness profile of the prepared layers, as obtained from the micrograph and histogram, revealed the thickness to be ~10 nm, thereby suggesting the exfoliation of bulk graphite. In order to further characterise the exfoliated graphene samples, Raman and TEM analyses were performed. The obtained Raman spectra, Fig. 1(e), suggested the exfoliation of yeast-treated graphite as indicated by the peak at 1350 cm^{-1} and ~ 2700 cm^{-1} corresponding to

D and 2D bands of few-layer graphene, respectively. The finite D peak for the yeast treated precursor is owed to the functionalization of prepared sheets due to functional groups introduced during yeast mediated exfoliation.[6] The 2D band at 2700 cm^{-1}, on the other hand, corresponds to the number of layers in the graphene and intensifies with decreasing number of layers.[7] The TEM micrograph, Fig. 1 (f), of the graphene suspension further demonstrated the presence of a few layer graphene flake in the dispersion.

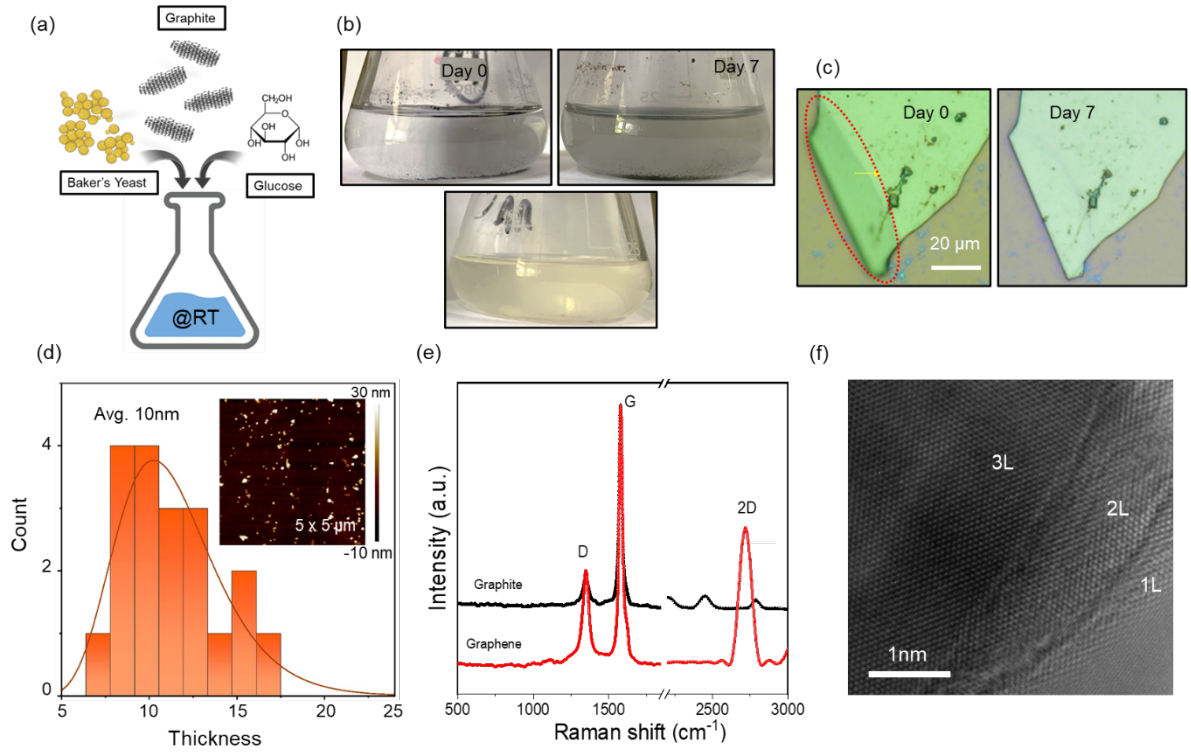

Fig 1: (a) Schematic of yeast-mediated exfoliation of graphite at room temperature in the presence of glucose, (b) photograph of the graphite in yeast and glucose solution on day 0 and day 7. The bottom image is a photo of the control sample with yeast fermenting glucose solution without graphite. (c) Optical micrograph of an anchored thin graphite flake (light green colour) on an oxidised silicon substrate with a few-layer graphene at the edge on Day 0 (pointed by the red dotted oval). After immersing in yeast-glucose solution, the few-layer graphene was found to be disappeared due to exfoliation. (d) Histogram of the thickness distribution of the exfoliated flakes obtained after keeping graphite in yeast and glucose solution for one week measured in AFM. Inset is an AFM image of the drop casted dispersion after differential centrifugation (e) Raman spectrum for graphite and graphene (before and after exfoliation) and (f) TEM image showing the presence of one, two and three layers of graphene at the edge of a few layer flake.

The exfoliation mechanism was studied using microscopic techniques including AFM and SEM, given in supplementary Fig. 1 and 2. The SEM micrographs suggested the yeast cells' attachment to the carbon layers where the shearing and tearing of the sheets was mediated by the growth and reproduction of the attached cells which occurs asexually through budding in case of *Saccharomyces cerevisiae*.[8] The separation of a daughter cell from the mother cell is hypothesised to result in layers dissociation and the formation of few-layer graphene structures.

The cell growth based AFM micrographs confirmed the exfoliation to be controlled by yeast cell growth where the graphite was considerably thinned down to few layers within few days of incubation. In addition, we suspect that the exfoliation will continue if thinner flakes are subjected to a fresh growing yeast. The thickness-to-time plot revealed a significant reduction in the thickness within 4 hours of incubation which corresponded to the logarithmic growth phase of dry yeast cells (Supplementary Fig. 2 (c)). Further thinning of the sheets was observed where the reduction was observed to reach ~10 nm in one week. The uniformity of the exfoliation process was established by estimating the standard deviation in the thickness of the prepared graphene with respect to incubation time where increasing incubation time led to the exfoliated structure with comparable thickness. The action of yeast cells on the edges of the prototype, graphite, was examined by studying the lateral dimension and aspect ratio of the exfoliated structure with respect to increasing incubation time with yeast cells, Supplementary Fig. 2 (d). The lateral dimension of the obtained layers was significantly reduced with increasing time which suggests the tearing the graphite from the edges by the yeast cells as shown in SEM micrographs. The aspect ratio of the obtained exfoliated flakes was observed to be increasing for up to 6 h of incubation. This indicated the formation of extremely thin graphene structure suggesting higher rate of thinning from within the layers of graphite in comparison to rate observed for delayering from the edges (out of plane for [001]). The observation can be attributed to the feasibility in overcoming the Van der Waals bonding in comparison to covalent bonding. The TEM analyses of the prepared few layer graphene has been elaborated in the supplementary section, supplementary Fig 3.

The functional and optical characterization of the exfoliated graphene layers was revealed by spectroscopic analyses. The UV absorption study of the prepared graphene, Fig. 2(a), demonstrated a characteristic peak at ~270 nm, assigned to $\pi \rightarrow \pi^*$ transition of aromatic C–C bonds.[9] The spectra were monitored with respect to the incubation period which showed the highest absorption to occur after 1 week of incubation with yeast cells, confirming the AFM analyses. The surface functionalization state of the obtained graphene flake was studied using FTIR and shown in Fig. 2(b). The distinct peaks were obtained at ~1630 and 1210 cm^{-1} which corresponded to the functional groups i.e., carboxylic and phosphate groups arising from yeast cell wall, thus suggesting the yeast cells based functionalization of the exfoliated graphene.[10] Post functional state analyses with FTIR spectroscopy, the exfoliated graphene was further characterized using Raman spectroscopy to identify the impact of yeast cells' growth parameters on its lattice and structural properties. The yeast cells' concentration in the suspension for graphite thinning was optimized by plotting the Raman spectra, Fig. 2 (c), for a

range of yeast cells' concentration (0-0.5% (w/v)). The significant change in the integrated area ratio (A_D/A_G) suggests the presence of functionalized graphene sheets owed to the yeast cells mediated exfoliation of graphite into graphene as already been established by FTIR study. However, for increased cells' concentration, the cell suspension was observed to be accrued with yeast cells forming a biofilm on the surface and impeding the aeration thereby limiting the cell growth. Therefore, the yeast cell concentration is considered to be a trade of exfoliation efficacy *versus* functional cell growth. Ordinarily, the transition from bulk to few layer carbon sheets results in the significant changes in the Raman spectroscopy parameters such as D/G, FWHM and band positions which directly correspond to functional and lattice state of the exfoliated sheets. Therefore, the incubation time (cell growth) based Raman spectra were obtained with incubation intervals of 0 min, 6 h, 1 day, and 1 week (supplementary file, Figure 4). The change in the G peak position and integrated area ratio (A_D/A_G) with respect to incubation time is shown in Fig. 2 (d).

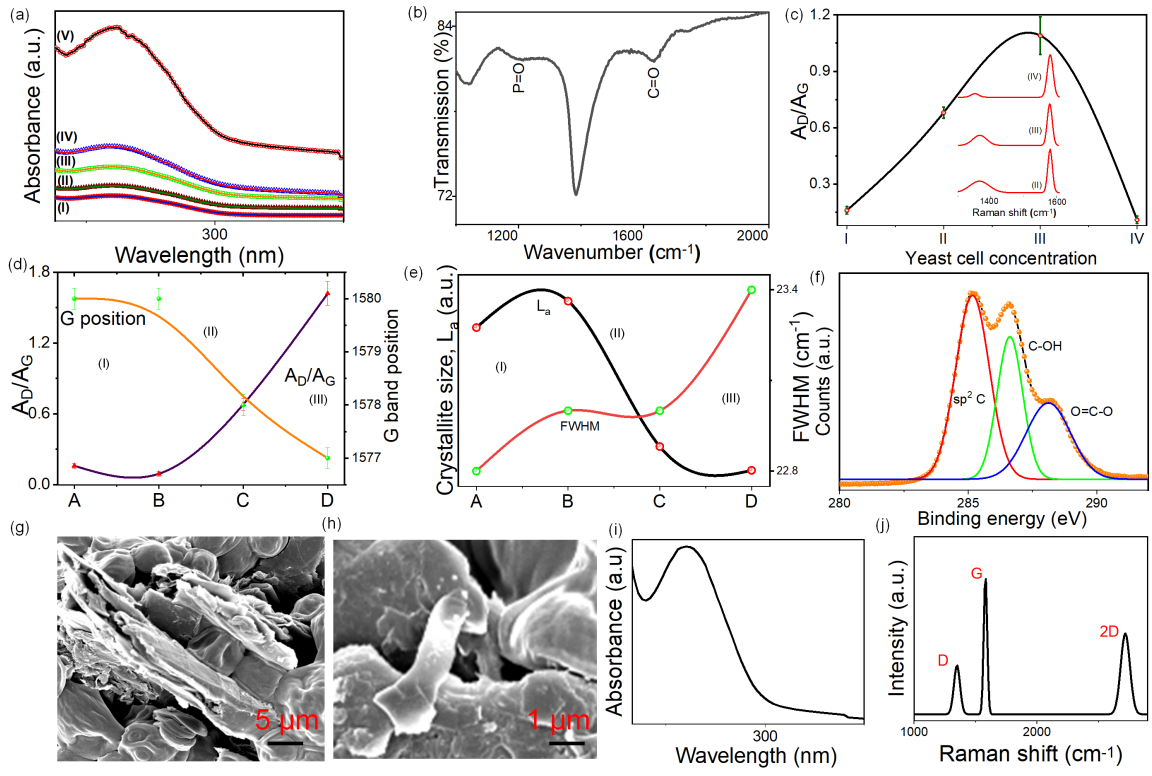

Fig. 2: (a) Time dependent UV-Vis spectra for (I), (II), (III), (IV), and (V) defined as 0 min, 1h, 6 h, 12 h, and 1 week respectively, (b) FTIR spectra for obtained graphene suspension, (c) A_D/A_G plot with respect to yeast cells concentration with (I), (II), (III), and (IV) defined as 0, 0.02, 0.2 and 0.5 % respectively, (d) A_D/A_G and G band position plot with respect to yeast cells incubation period, (e) FWHM and L_a with respect to incubation period with (A), (B), (C), and (D) defined as 0 min, 6 h, 1 day and 1 week respectively, (f) High resolution XPS survey obtained for C 1s and (g and h) SEM scans of exfoliated graphite, (i and j) UV-Vis and Raman spectrum for graphene obtained at 50° C Incubation

The red shift in the G band suggests the presence of strained sheets,[11] which can be due to the stretching of the sheets by the yeast cells leading to elongated C-C bonds (supplementary Fig. 2). Further, the A_D/A_G ratio, influenced by the functionalization of the prepared structure, was found to increase with increasing incubation time. The spectra, obtained for 0 min of incubation time, exhibited a feeble D peak suggesting the precursors to be free of defects. The intensification of the D band with increasing incubation time is attributed to the functionalization of the edges owing to the yeast cells driven exfoliation.[6] The A_D/A_G ratio was further explored to evaluate the in plane sp^2 crystallite size, L_a, according to the relation given by Cançado *et al.* for graphitic materials, wherein L_a was reported to be inversely proportional to A_D/A_G.[12] The relative L_a was plotted with respect to incubation time as shown in Fig. 2 (e). The plot suggests the gradually decreasing lateral dimension of the exfoliated graphene for up to 1 week of incubation. The obtained pattern was found to be in agreement with the changes observed in the lateral dimension of the layers from AFM micrographs (Supplementary Fig. 2 (e)). The FWHM value for the G band suggested the formation of exfoliated structure as higher G_{FWHM} corresponds to increased interlayer spacing (d_{002}).[13] Fig. 2 (e) shows the change in the FWHM with incubation time where the value was found to be gradually increasing with increasing time and hinted at the disruption of graphite for the formation of few layer graphene. The elemental survey of the exfoliated graphene revealed the presence of C, O and N atomic states. The XPS spectra of C 1s, (Fig. 2 (f)), with deconvoluted peaks at ~ 284.8 eV, 286 eV and 288 eV are assigned to sp^2 C carbon, C-OH and O=C-O.[14] The presence of oxygen containing functional groups in C 1s spectra due to the yeast cells in the graphene suspension. Based on the changes observed for A_D/A_G, L_a, the G band position and the FWHM values with respect to incubation time, the exfoliation process can be divided into three stages (attachment, division and separation of yeast cells) to elucidate the step wise thinning of graphite. The attachment phase (I), Fig. 2 (g), starts immediately after incubation and as observed from the plots, there are no significant changes in the lattice parameters during this stage. The attachment stage often overlaps with the cell division, where the attached cells begin to divide causing the shearing and tearing of the substrate (graphite), significant changes in the lattice parameters were observed at the second stage of exfoliation. Further, the stage III is characterized by the separation stage, which is marked with the cell division phase and is completed within 1 weeks of incubation, Fig. 2(h).

In order to detect the impact of elevated temperature on the exfoliation process, the reaction mixture was incubated at 50° C for 1 week. The increased temperature was expected to increase

the reaction rate without impacting the yeast cells' growth. The obtained exfoliated structure was examined using spectroscopic techniques to determine its impact on the exfoliation process. The UV-Vis absorption spectrum and the Raman spectrum indicated no significant changes in the exfoliation yield and lattice properties of the obtained exfoliated structure for incubation at higher temperature.

To gain further insight into the mechanism of yeast-assisted exfoliation of graphite as a function of time using fully atomistic Molecular Dynamics (MD) simulations. Here, we discussed the role of thickness in exfoliating graphene sheets. To this end, we initially considered two layers of graphite (area = 30 Å x 25Å) without any defect which were confined between two cell membranes of the yeast cell, modelled as a phospholipid bilayer made of phosphatidylcholine (POPC) molecules (see methodology and supplementary section for details) at t=0 ps, as shown in Fig. 3 (a). Within t=16 ps of simulation time (Fig. 3 (b and c)), The two-layers separation suggests that graphite-yeast interaction to be sufficiently strong to completely overcome the inter-graphite sheets Van der Waals (VdW) interactions.

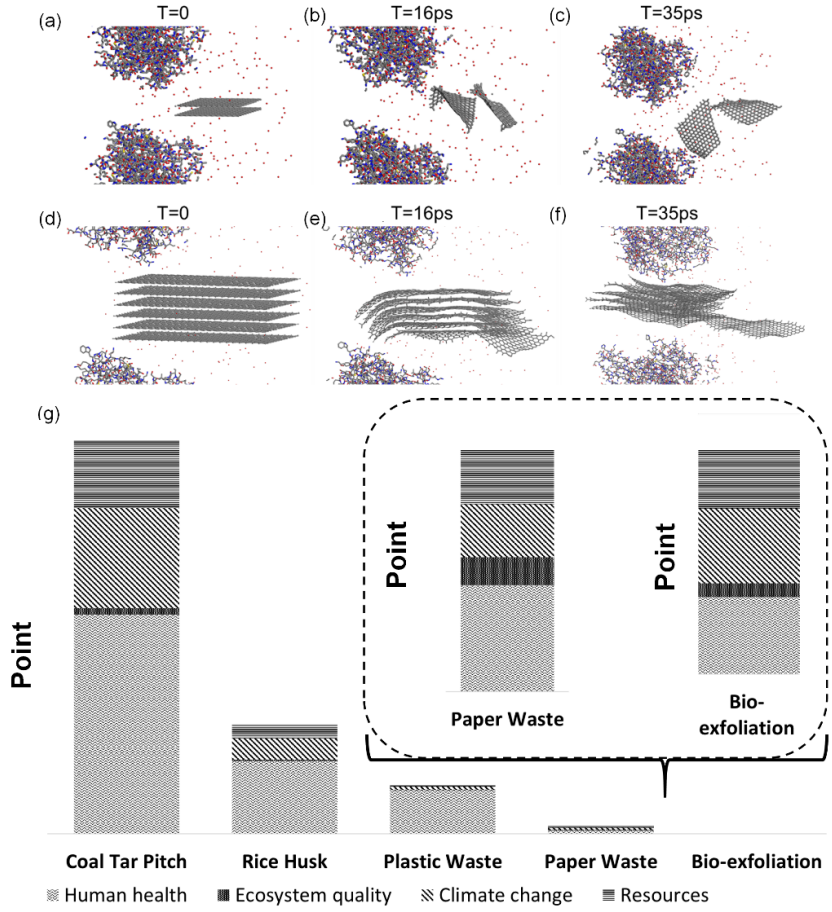

Fig. 3: Simulated exfoliation of graphene from yeast. Representative MD snapshots of the yeast and graphene layers at different simulation time for (a-c) two layers (d-f) six layers. Initial structure at T=0ps and intermediate structure at T=16ps, 35ps, where graphene starts exfoliating; (g) Comparative life cycle assessment of graphene production routes, see text for discussions

198 Similarly, we also considered six parallel graphite layers (area = 40 Å x 70 Å) shown in Fig. 3
199 (d), to determine whether the layer separation could also occur for thicker structures. As
200 observed for two-layer case, within t=16 ps of simulation time, layers started to separate,
201 showing again that the graphite/yeast interactions are strong enough to overcome the Van der
202 Waals forces of thicker layers. This phenomenon was supported by Fig. 3 (e and f), the
203 concentration profile of the graphene corresponding to the [0 0 1] direction shows that the
204 confined fluid has a higher density closer to the membrane surfaces indicating the sticking to
205 be mediated by shear stress. The yeast sticking phenomena of six layer is slightly higher in
206 comparison to two-layers, this can be attributed to the higher surface area. In summary, the
207 MD results further support that the yeast-membrane interaction with graphite are sufficiently
208 strong to wet its surface and induce exfoliation by shear stress, even considering the thicker
209 graphite structures (further details given in the supplementary file).
210 A stand-alone LCA was performed using the yeast driven-exfoliation process experimental
211 data to identify the potential environmental hotspots by extrapolating the laboratory-scale data
212 to a hypothetical commercial scale (system boundary and other details have been provided in
213 the supplementary section). The outcomes significantly depend upon scale, production routes
214 and energy mix. Environmental profiles for end point characterization of the graphene
215 production are shown in Fig. 3 (g). Overall, de-ionized water (36.11%), electricity production
216 (35.41%) and glucose production (26.57%) were identified as environmental hot-spots in the
217 bio-exfoliation process. The electricity production is identified as the major contributing
218 emission towards human health while de-ionized water production contributed to both climate
219 change and resource depletion. Overall, the bio-exfoliation production route is established as
220 the green process compared to other approaches involving coal tar, rice husk, plastic waste and
221 paper waste. Thus, the shift towards using renewable-based energy sources provides a
222 promising route towards the reduced ecological impacts in the current geographical context.
223 The acid-base homeostasis in a human body is maintained by the kidneys, which eliminate the
224 acid (H^+) in the form of NH_4^+ through excretion. Low ammonium excretion is associated with
225 the impaired ability of the kidneys to remove the acids which is classified as chronic kidney
226 disease (CKD and further linked to an elevated risk of end-stage renal disease (ESRD), acidosis
227 and kidney failure.[15] Hence, monitoring the ammonium excretion level in patients at early
228 stages is effective to circumventing the occurrence of such unlikely clinical events. Previous
229 studies reported the utilization of graphene for ultra-low detection of ammonia (NH_3), where
230 graphene sheets were functionalized to fabricate a nanocomposite film as sensor.[16–18]
231 However, in the present study, the bio-prepared few-layer graphene exhibited the presence of

residual functional groups as shown in the FTIR study, which can effectively provide sites for NH_4^+ absorption or binding, without requiring further post-synthesis modification.[19] Therefore, as-prepared few-layer graphene were explored for their use in low-level sensing of NH_4^+ ions (sensing mechanism shown in Fig. 4 (a)). The binding of ammonium ions to graphene sheets was examined using UV-Vis spectroscopic analyses. The change in UV-Vis spectra of graphene was recorded for different concentrations of NH_4Cl solution as shown in Fig. 4 (b). The absorption plots demonstrated a smooth decline in the characteristic absorbance peak at ~270 nm with the increasing amount of analyte, NH_4^+, which suggests the binding of ammonium ions to few-layer graphene. In order to further investigate the UV absorption behaviour of few-layer graphene in the presence of NH_4^+ ions, the absorbance with increasing analyte amount (0.5 mM up to 3.75 mM) was plotted for different graphene amount (G-I to G-V) (Fig. 4 (c and d)). Here, I to V define the increasing concentration of few-layer graphene, i.e., from 0.06% up to 0.15% (v/v). The change in the absorption was quantified and plotted with respect to NH_4^+ ions concentration for elucidating the binding affinity and saturation conditions. The most significant reduction in the absorption was found to be for the graphene concentration of 0.1% (v/v) which suggested the most effective binding and ammonium absorption at the particular concentration. In Fig. 4 (e), G-III showed a linear decline in the absorbance with NH_4^+ concentration, which was fitted to establish a linear relationship between absorbance changes and ammonium concentration. The calibration curve was further explored to estimate the limit of detection (LoD) and the limit of quantification (LoQ). The detection limit indicated the lowest concentration of ammonium ions which was detected by few-layer graphene and was found to be ~20 ppm, while the quantification limit was estimated on the basis of repeatability and precision and was calculated to be 1.8 mM. Further, the association between the analytes and detector i.e. NH_4^+ ions and graphene respectively was studied using the Benesi-Hildebrand equation, Fig. 4 (f), which estimated the binding constant (K_b) to be ~ 0.6×10^3 M^{-1}. The low value of the binding constant suggested the moderate binding as reflected by the estimated LoD and LoQ values. The affinity between the prepared few-layer graphene and analyte, ammonium ions, is ordinarily governed by a plethora of factors i.e. the number of layers in the graphene, the presence of surface groups, etc. The comparative plot was drawn to collate the ammonium ions detection carried out by graphene sheets. Here, the biologically prepared few-layer graphene demonstrated a detection limit of 20 ppm which was comparable to that observed in previous reports, Fig. 4 (g).[17,18,20]

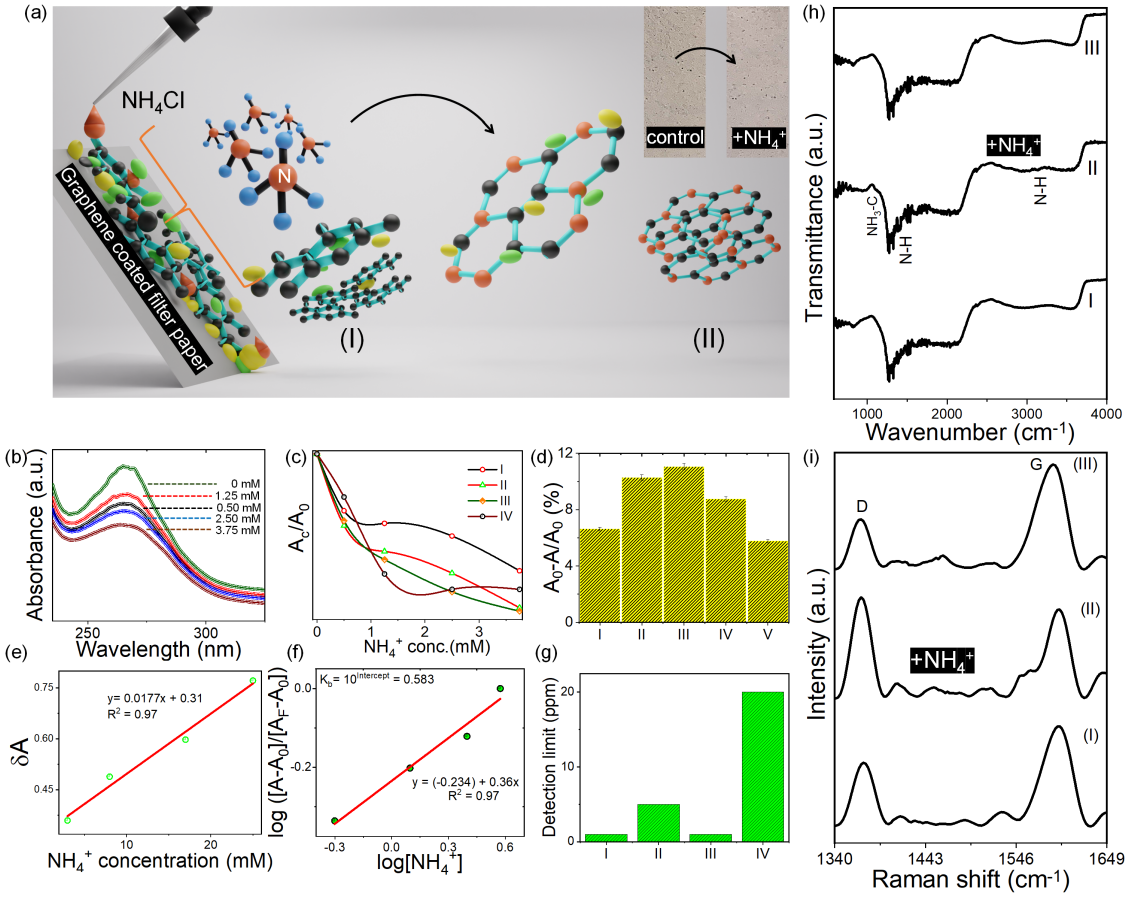

Fig. 4: (a) schematic for NH_4^+ ions sensing by graphene layers where (I) and (II) signify the binding and incorporation of N atoms in the carbon hexagonal lattice, (b) change in the UV Vis absorption spectra for graphene with NH_4^+addition, (c) decreasing absorbance for graphene solution at different concentration (I to V), (d) relative change in absorption plots with respect to graphene concentration, (e) calibration curve for change in absorption with respect to ammonium ions concentration, (f) Benesi–Hildebrand plot for determination of binding constant of graphene for ammonium ions, (g) the comparative plot with ammonium detection for graphene prepared using different methods I: chemiresistive graphene, II: hydrazinium graphene (HG) prepared from exfoliated graphene oxide, III:chemically derived graphene, IV: functionalized graphene (present work), (h) FTIR spectra for I, II, and III i.e. control, ammonium treated, and heated graphene suspension, (i) Raman spectra for I, II, and III i.e. control, NH_4^+ ions treated, and heated graphene suspension.

In order to gain further insights into the sensing mechanism, control and ammonium treated graphene samples were examined for the changes in their surface chemical state and lattice structure using FTIR and Raman spectroscopy (Fig. 4 (h and i). Here, the reproducibility of the system was checked by heating the ammonium treated graphene and examining the changes using spectroscopic techniques. The FTIR peaks revealed the changes in the surface chemical composition of the graphene sheets upon NH_4Cl application. From the plot, Fig. 4(h), there are significant changes observed in the NH_4^+ treated graphene, in comparison to control and heat treated graphene-NH_4^+. The peaks at ~3100 and ~1400 cm^{-1}, observed for ammonium treated graphene, correspond to N-H stretching and bending respectively. Further, the band at ~1090 cm^{-1} corroborates to the symmetric NH_3 signifying the coordination of NH_3 to Lewis acid sites on the carbon surface (graphene layers).[21] The peak at ~820 cm^{-1}, assigned to the deformation vibration for C-H groups in carbohydrates, i.e., glucose here, was observed to be absent for

NH_4^+ treated graphene suspension. The absence of peak can be owed to the glucosamine formation, where hydroxyl group at the anomeric carbon can be replaced with an amine group. Therefore, the FTIR examination confirms the binding of ammonium ions to the carbon atoms in the graphene structure. The binding was further validated by Raman spectroscopic analysis where the control and treated samples were studied for the changes in the edge defects, disorder and functional groups. The plots demonstrate the significant changes in the graphene layers upon NH_4^+ incorporation, which was inferred by increasing A_D/A_G. The obtained results suggested the formation of C-N bonding and incorporation of nitrogen atom in the hexagonal lattice thereby leading to functionalization. The FTIR and Raman behaviour of the heat treated samples revealed that changes, observed in the ammonium treated graphene samples, were found to be absent in the heated samples, which marks the reproducibility of the bioprepared graphene as ammonium ions sensor. Hence, the biopreparation of graphene layers can be useful for real life application in ammonium ions sensing in human urine to detect the changes due to kidney dysfunctionality.

Conclusion

Here, we have presented a method to bio-exfoliate graphite sheets into few-layers graphene, which was elucidated using different structural and spectroscopic analyses. The changes in the thickness reduction were thoroughly examined using AFM, which suggested the reduction to ~10 nm thickness in one week of incubation and Raman spectroscopy also validated the formation of few-layers graphene structures. The IR spectroscopic examination revealed the presence of functional groups on the prepared graphene which enabled its application for the ammonium ions sensing via UV-Vis absorption spectroscopy with LoD to be 20 ppm. The affinity of the yeast cells for graphene was studied using molecular dynamics simulation which suggested the exfoliation results from shear stress induced by the yeast and the yield to be determined by the thickness and surface area of graphite. In summary, we present a new bio-exfoliation method to obtain few-layers graphene from graphite. The method is very simple and it uses widely available yeast cells. It is non-expensive, green and scalable (industrial scale). In principle, it can be used to exfoliate other layered materials (as demonstrated for MoS_2 in the supplementary data), which opens new perspectives to obtain and use few-layer structures.

Methods

Yeast mediated exfoliation of graphite

Dry yeast cells (0.2% (w/v)) were incubated with graphite containing glucose solution (0.5% (w/v)). During the experiment, the yeast cells could reach and remain in the stationary phase of growth. The visual change in the yeast containing solution was the first indication of exfoliation of graphite.

Characterization of the exfoliated graphene

Differential centrifugation in the steps of increasing RPMs from 4k (allowing yeast and larger graphite chunks), followed by subjecting the supernatant to 14k RPM in 2 steps to collect the precipitate with smaller exfoliated flakes. The precipitate or the pellet is diluted and rinsed in water. It is further drop-casted on Si substrates with 300 nm SiO2 Height and surface profiles of as prepared graphene sheets were studied using Atomic Force Microscopy (AFM, Agilent Technologies, USA, Model 5100). All the measurements were carried out in air at room temperature (25º C) using a Silicon Nitride Tip (PPP-NCL) in the intermittent contact mode. The Scanning Electron Microscope (SEM) micrographs of graphene were obtained with ZEISS EVO 60 Scanning Electron Microscope with an Oxford EDS detector. The phase and lattice characterization of the bio-exfoliated graphene sheets was carried out using powder X-Ray Diffraction (XRD) with monochromatic nickel filtered Cu Kα radiation in the 2θ range of 20 to 80˚. The optical spectra of the prepared samples were recorded using a UV-1800 spectrophotometer, Shimadzu, Japan. The High Resolution- Transmission Electron Microscopy (HR-TEM) images were produced using JEOL 2200FS electron microscope. The Fourier Transform Infrared (FTIR) analysis of graphene was carried out using Bruker spectrometer through the range of 4000 to 400 cm^{-1}. The Raman spectra of graphene sheets were acquired with an excitation wavelength of 532 nm (Witec UHTS 300). X-ray photoelectron spectroscopy (XPS) measurements were performed with Thermoscientific spectrophotometer (NEXSA) with a micro focused monochromatic Al-K_α source (1486.6 eV).

Computational study methodology

To theoretically evaluate the structural stability of few-layers graphene and/or graphene/yeast membrane cells, we carried out fully atomistic Molecular Dynamics (MD) simulations, as implemented in the open-source code LAMMPS.[22] The well-known Universal Force-Field (UFF) formalism was used to calculate the interatomic interactions and/or configurational energies.[23] For creating the simulation box, initially, a supercell of 50 Å x 80 Å x 135 Å was created that includes a 20 Å vacuum along with two layers of graphite confined between

membrane yeast cells. 20 Å buffer vacuum was used to avoid spurious interactions of the supercell replication. Another supercell was created with the same dimension for the six-layers graphite structure. As discussed above, this was used to determine the thickness relationship with the exfoliation mechanism contributing to yield. The outer cell membrane of the yeast is modeled as a phospholipid bilayer made of phosphatidylcholine (POPC) molecules commensurate with the dimensions of the graphene-layered structures. The structural data of the models are available upon request. For performing the simulations on the layered structures, a variable cell relaxation calculation was performed to equilibrate the yeast cell layers by constraining the graphite layers and to eliminate any bad contacts generated from the layer/membrane building processes. To further avoid any residual structural stresses, NVT equilibration MD runs were performed during 100 ps. Finally, the confined shear simulations were performed to examine the exfoliation mechanism by removing the constraints from graphite layers, setting wall velocity (U) to 5Å/ps and simulation time (t) as 100ps. This kind of simulation protocol has been extensively used in the literature.

Life cycle assessment methodology

The environmental impacts of graphite exfoliation using biological synthesis were quantified using the life cycle assessment (LCA) approach as per ISO 14040–44 (ISO 14040, 2006; ISO 14044, 2006). Four steps were involved in the process (a) goal and scope definition, (b) life cycle inventory (LCI), (c) life cycle impact assessment (LCIA), and (d) life cycle interpretation. This study's primary goal is to evaluate environmental impacts of graphite exfoliation using biological synthesis. The scope of this LCA includes only the exfoliation of graphite into few-layers graphene (gate-to-gate). The upstream life cycle stages utilization of graphene and disposal stages were excluded. The energy calculations were performed using specific heats of materials and/or the power rating of the equipment used in the synthesis process. The location of graphite exfoliation plant was considered Kharagpur, India, the source of materials and chemicals was based on the local conditions (Kolkata, India). The eastern India electricity power mix was used for energy consumption. The study’s functional unit was the exfoliation of 1 ton of graphite. The functional unit was chosen to compare the feasibility of producing graphene from waste-based feedstocks from an environmental perspective at an industrial scale. The parameters and components in synthesis routes for graphite exfoliation were scaled to the industrial level and were normalized to the functional unit. The scaled-up quantities of materials and amount of energy were normalized to the functional unit, assuming that reaction rates remain unaltered at the industrial scale. Environmental impacts were evaluated using

SimaPro 8.0.3 version software and Eco-invent database. IMPACT 2002+® method was used for the characterization of end-point impacts. Since we are aiming to study the industrial-scale exfoliation of graphite, we choose the process contributions which are most relevant to the production processes. Sensitivity analysis was performed by varying the country's electricity mix and quantity of deionized water. In the present investigation, a high-voltage electricity grid mix of the Indian geographic location was used for modeling the scenarios. For sensitivity analysis, the electricity mix of China and Norway was modeled to compare and evaluate the impacts associated based on the shift towards reduction in the coal-based electricity mix. Comparative LCA was performed with graphene production routes using (a) coal-tar pitch; (b) Rice-husk; (c) Plastic waste; and (d) Paper Waste.

Ammonium ions sensing experiments

The bioprepared graphene sheets were checked for NH_4^+ sensing *via* UV-Vis absorption spectroscopy, where graphene suspension was mixed with NH_4Cl solution at different concentrations (0.5 -3.75 mM). The change in the absorbance was quantified, and the calibration plot was obtained to estimate LoD and LoQ. Further, to comprehend the sensing mechanism, control and ammonium-treated graphene were examined under Raman and FTIR spectroscopy for changes in the surface chemical state and lattice structure introduced by NH_4^+ ions.

Email address of the corresponding authors:
Prof. Chandra Sekhar Tiwary: cst.iisc@gmail.com
Prof. Rahul R Nair: rahul@manchester.ac.uk
Prof. Rintu Banerjee: rb@iitkgp.ac.in

Acknowledgement

The authors acknowledge the Central Research Facility of the Indian Institute of Technology, Kharagpur, for providing high-end instruments required in the sample analysis. We also acknowledge Advanced photonics lab, Department of Electronics and Electrical Communication Engineering, IIT Kharagpur for FTIR measurements. DSG acknowledges support from FAPESP/CEPIP grant 2013/08293-7.

1. Zhang, Y., Zhang, L. & Zhou, C. Review of chemical vapor deposition of graphene and related applications. *Acc Chem Res* **46**, (2013).
2. Li, X. *et al.* Large-area synthesis of high-quality and uniform graphene films on copper foils. *Science (1979)* **324**, (2009).
3. Zavabeti, A. *et al.* Two-Dimensional Materials in Large-Areas: Synthesis, Properties and Applications. *Nano-Micro Letters* **12**, (2020).
4. Meyers, M. A., Chen, P. Y., Lin, A. Y. M. & Seki, Y. Biological materials: Structure and mechanical properties. *Progress in Materials Science* **53**, (2008).
5. Csuk, R. & Glänzer, B. I. Baker's Yeast Mediated Transformations in Organic Chemistry. *Chem Rev* **91**, (1991).
6. Sharma, R., Baik, J. H., Perera, C. J. & Strano, M. S. Anomalously large reactivity of single graphene layers and edges toward electron transfer chemistries. *Nano Lett* **10**, (2010).
7. Ferrari, A. C. & Basko, D. M. Raman spectroscopy as a versatile tool for studying the properties of graphene. *Nature Nanotechnology* **8**, (2013).
8. Willey, J., Sherwood, L. M. & Woolverton, C. J. Microbiología de Prescott, Harley y Klein. **4**, (2009).
9. Alanyalioğlu, M., Segura, J. J., Oró-Sol, J. & Casañ-Pastor, N. The synthesis of graphene sheets with controlled thickness and order using surfactant-assisted electrochemical processes. in *Carbon* **50**, (2012).
10. Fan, H. *et al.* Fabrication, mechanical properties, and biocompatibility of graphene-reinforced chitosan composites. *Biomacromolecules* **11**, (2010).
11. Ni, Z. H. *et al.* Uniaxial strain on graphene: Raman spectroscopy study and band-gap opening. *ACS Nano* **2**, (2008).
12. Cançado, L. G. *et al.* Disentangling contributions of point and line defects in the Raman spectra of graphene-related materials. *2d Mater* **4**, (2017).
13. Yoshida, A., Kaburagi, Y. & Hishiyama, Y. Full width at half maximum intensity of the G band in the first order Raman spectrum of carbon material as a parameter for graphitization. *Carbon* **44**, (2006).
14. Siokou, A. *et al.* Surface refinement and electronic properties of graphene layers grown on copper substrate: An XPS, UPS and EELS study. *Appl Surf Sci* **257**, (2011).
15. Adeva, M. M., Souto, G., Blanco, N. & Donapetry, C. Ammonium metabolism in humans. *Metabolism: Clinical and Experimental* **61**, (2012).
16. Ghosh, R. *et al.* Highly sensitive large-area multi-layered graphene-based flexible ammonia sensor. *Sens Actuators B Chem* **205**, (2014).
17. Mackin, C. *et al.* Chemiresistive Graphene Sensors for Ammonia Detection. *ACS Appl Mater Interfaces* **10**, (2018).
18. Wu, Z. *et al.* Enhanced sensitivity of ammonia sensor using graphene/polyaniline nanocomposite. *Sens Actuators B Chem* **178**, (2013).
19. Yang, Y. *et al.* In situ polymerization deposition of porous conducting polymer on reduced graphene oxide for gas sensor. *ACS Appl Mater Interfaces* **6**, (2014).
20. Fowler, J. D. *et al.* Practical chemical sensors from chemically derived graphene. *ACS Nano* **3**, (2009).
21. Zawadzki, J. & Wiśniewski, M. In situ characterization of interaction of ammonia with carbon surface in oxygen atmosphere. *Carbon N Y* **41**, (2003).
22. Prieve, D. C. & Russel, W. B. Simplified predictions of Hamaker constants from Lifshitz theory. *J Colloid Interface Sci* **125**, (1988).
23. Rappé, A. K., Casewit, C. J., Colwell, K. S., Goddard, W. A. & Skiff, W. M. UFF, a Full Periodic Table Force Field for Molecular Mechanics and Molecular Dynamics Simulations. *J Am Chem Soc* **114**, (1992).